

properties (use the SMA austenite yield strength and the SMA modulus of elasticity). Only for a preliminary design under the load combination of “Extreme Event I”, the AASHTO response modification factors (AASHTO LRFD⁴⁹, Table 3.10.7.1-1) may be used to reasonably size the columns and the adjoining members. Nevertheless, SMA-reinforced ECC columns should be analyzed and designed according to the present guideline for seismic loads.

Details of SMA-Reinforced ECC Columns

The incorporation of ECC only over a partial length of columns should be permitted. The length of the ECC portion of columns in the plastic hinge region should be at least 1.5 times the largest column cross-sectional dimension.

The area of longitudinal reinforcing SMA bars (A_{SMA}) in the SMA-reinforced ECC columns should satisfy:

$$0.01A_g \leq A_{SMA} \leq 0.04A_g \quad (\text{Eq. 8})$$

where A_g is the gross area of member cross-section. Since the austenite yield strength of SMA bars is usually lower than the steel bar yielding, a higher amount of longitudinal reinforcement than conventional columns is expected, but the reinforcement area should be within in the specified range. NiTi SE SMA bars are available from No. 4 (13 mm) to No. 18 (57 mm).

The incorporation of SMA bars only over a partial length of columns should be permitted and recommended to save cost. The length of SMA bars should be the greater of (a) the analytical plastic hinge length (**Eq. 2**), and (b) 75% of the largest column cross sectional dimension ($0.75D$). The $0.75D$ limit was based on an experimental study using two SMA bar lengths in the plastic hinge region. The column with the shorter SMA bars exhibited a lower drift capacity³².

SMA bars are plain (with smooth surface) behaving similarly to debonded bars under cyclic loading. When SMA bars are used over the entire length of members, mechanical anchorage should be used to anchor the bars in the adjoining members. When SMA bars are utilized only in the plastic hinge region, reinforcing SMA bars should be connected to reinforcing steel bars using mechanical bar splices approved by the bridge owner. SMA bars spliced with threaded (only those with parallel threads but not those with tapered threads) and headed bar couplers have shown large strain capacities. Furthermore, large-scale SMA-reinforced columns incorporating these coupler types exhibited satisfactory performance under static and dynamic loads e.g.^{24, 38}. **Figure 11** shows the headed bar splice developed for SMA bars. Splicing should be permitted in the plastic hinge region of the columns pending the owner approval. The drift capacity of mechanically spliced bridge columns needs to be reduced based on the coupler type, size, and location following design methods proposed by Tazarv and Saiidi⁵⁰.

The axial load acting on an SMA-reinforced ECC column including gravity and seismic demands (P_u) where a pushover analysis is not performed should satisfy:

$$P_u \leq 0.15f'_{ECC}A_g \quad (\text{Eq. 9})$$

where A_g is the gross area of member cross-section and f'_{ECC} is the nominal ECC compressive strength. A higher axial load value may be used provided that a pushover analysis including the $P - \Delta$ effect is performed to compute the maximum drift capacity of the column. The aspect ratio of SMA-reinforced ECC bents should not exceed eight. Columns with larger aspect ratios may fail at low drift ratios due to the $P - \Delta$ effect.

FIELD APPLICATION

The world first NiTi SMA-reinforced ECC bridge, the SR99 Alaskan Way Viaduct Bridge, was constructed in 2017 in Seattle, WA (**Fig. 12**). The three-span bridge was 400-ft (120-m) long and 30.5-ft (9.30-m) wide with precast post-tensioned concrete spliced tub girders. The length of the middle span was 180 ft (55 m) and the two end spans were each 110-ft (34-m) long.

The superstructure was supported by two single-column bents. Each column had a square cross-section with a side dimension of 5 ft (1.5 m) reinforced with SMA and steel bars in a circular pattern (**Fig. 12a**). Longitudinal No. 10 (32-mm) SMA bars each 4-ft (1.22-m) long were used at the top plastic hinge of the columns and No. 10 (32-mm) steel bars were used elsewhere as the longitudinal bars. SMA bars were connected to steel bars through headed reinforcement couplers (**Fig. 11 & 12b**). The SMA bars were used only at the top of the column due to the soil condition of the site, which was prone to liquefaction. ECC was also used only in the top plastic hinge region with a total length of 5 ft (1.5 m). Complete details of the bridge can be found in Baker et al.⁵¹.

The full version of the guidelines presented in this document was not available at the time of the design of the SR99 bridge. However, the SMA material model and expected material properties (**Fig. 1** and **Table 1**) were available and were used in the design of the SR99 bridge columns. The length of the SMA bars in the plastic hinge region, which was 80% of the column side dimension, was determined through testing of three 33%-scale columns detailed based on the prototype SR99 columns. One conventional column was built with steel bars and concrete to serve as the reference model, and two columns were constructed using SMA bars and ECC in the plastic hinge region (**Fig. 12b**). The only difference between the two SMA column models was the length of SMA bars. One was built with 20-in. (508-mm) long SMA bars (equal to the test column side dimension) and another column was built with 15-in. (380-mm) long SMA bars (75% of the column side dimension). Since both SMA-reinforced ECC columns showed better seismic performance compared with the reference column, the shortest SMA bar length was used in the field with a slight increase (from 75% of the column side dimension to 80%). Complete detail of the column test results can be found in Nakashoji and Saiidi³². The SR99 bridge is expected to remain fully functional with minimal damage after a severe earthquake.

CONCLUSIONS

Novel bridge columns are emerging to enhance the seismic performance of bridges by reducing the damage, increasing the displacement capacity, and/or reducing the residual displacement. Of the different novel columns, NiTi SMA-reinforced ECC bridge columns have gained a substantial momentum in the U.S. since they exhibit lower damage and insignificant residual displacements after strong earthquakes. The present study was performed to recommend a set of displacement-based design guidelines for this column type based on all available test data and extensive analytical studies. The key findings and recommendations are summarized as follows:

- A simple design equation was proposed to relate drift to ductility based on the analysis of approximately 700 bridge columns covering all practical ranges. It was found that the most important factor to relate drift to ductility is the column aspect ratio.
- The displacement demand of SMA-reinforced ECC bridge columns should be increased by 20% when the equivalent static or spectral analysis is performed using spectra provided by current codes. For linear or nonlinear dynamic analyses, the damping ratio of SMA-

reinforced ECC columns should be reduced from typical 5% to 3.2% to include the effect of flag-shaped behavior.

- Superelastic SMA bars usually show a trilinear stress-strain behavior. The design moment and shear forces for SMA-reinforced ECC columns should include the effect of the martensite modulus (k_3 in **Fig. 1**). Otherwise, the column force demands might be underestimated.
- The residual displacements of SMA-reinforced ECC columns are insignificant increasing the post-event functionality of the bridge.
- The displacement capacity of SMA-reinforced ECC columns are at least equal to that of conventional columns following the proposed limitations on the SMA length.

The available test data and analyses have confirmed an enhanced performance for SMA-reinforced ECC columns compared with conventional RC columns. The proposed guidelines were developed to facilitate the use of this type of novel column in the seismic regions of the nation.

Further research is mainly needed at the material level such as the establishment of material behavior for different SMA alloys, and the use of different ECC mixes and confining methods. However, the present guideline skeleton might be used for the development of design recommendations for different SMA and ECC types.

ACKNOWLEDGEMENTS

The research reported herein was performed under National Cooperative Highway Research Program (NCHRP) Project 12-101 by Infrastructure Innovation, LLC in collaboration with BergerABAM and Modjeski and Masters, Inc. Their support and feedback are greatly appreciated.

NOTATION

A_g	= The gross area of member cross-section (in ² or mm ²),
α	= The SMA secondary post-yield stiffness ratio,
A_{SMA}	= The area of longitudinal reinforcing SMA bars (in ² or mm ²),
A_r	= The column aspect ratio,
β	= The SMA lower plateau stress factor,
D	= The largest column cross sectional dimension (in. or mm),
δ	= The drift ratio (%),
δ_c	= The drift ratio capacity (%),
δ_D	= The drift ratio demand (%),
Δ_c	= The column displacement capacity (in. or mm),
d_{bl}	= The nominal diameter of longitudinal column reinforcing SMA bars (in.),
E_{ECC}	= The secant modulus of elasticity for ECC (ksi or MPa),
ϵ_r	= The SMA recoverable superelastic strain,
ϵ_u	= The ultimate strain,
f^{ECC}	= The nominal ECC compressive strength (ksi or MPa),
f_y	= The SMA austenite yield strength (ksi or MPa),
f_{ye}	= The expected austenite yield strength of the longitudinal column reinforcing SMA bars (ksi),
I_{eff}	= The effective moment of inertia (in ⁴ or mm ⁴),
L	= The column length (in. or mm),

- μ = The displacement ductility,
 μ_c = The displacement ductility capacity,
 μ_D = The displacement ductility demand,
 Ω = The deformability factor, 1.2 for SMA-Reinforced ECC columns,
 k_1 = The SMA austenite modulus (ksi or MPa),
 k_2 = The SMA post yield stiffness (ksi or MPa),
 M_p = the idealized plastic moment,
 M_u = The column failure moment,
 P_{dl} = The tributary dead load applied at the center of gravity of the superstructure (kips or kN),
 P_n = The nominal axial capacity of an SMA-reinforced ECC column,
 P_u = The axial load demand including gravity and seismic loads (kips or kN),
 V_c = The ECC contribution to the shear capacity,
 V_n = The nominal shear capacity of member,
 V_s = The reinforcing steel contribution to the shear capacity,

REFERENCES

- [1] FHWA Annual Materials Report, 2013, Retrieved May 9, 2019, from https://www.fhwa.dot.gov/bridge/nbi/no10/yrblt_yrreconst13.cfm.
- [2] Otsuka, K., and Wayman, C. M. "Mechanism of Shape Memory Effect and Superplasticity," Cambridge University Press, Cambridge, U.K., 1998, pp. 27-48.
- [3] DesRoches, R. and Delemont, M., "Seismic Retrofit of Simply Supported Bridges Using Shape Memory Alloys," *Engineering Structures*, V. 24, 2002, pp. 325-332.
- [4] Araki, Y., Endo, T., Omori, T., Sutou, Y., Koetaka, Y., Kainuma, R., and Ishida, K., "Potential of Superelastic Cu-Al-Mn Alloy Bars for Seismic Applications," *Earthquake Engineering and Structural Dynamics*, V. 40, No. 1, 2011, pp. 107-115.
- [5] Shrestha, K.C., Araki, Y., Nagae, T., Koetaka, Y., Suzuki, Y., Omori, T., Sutou, Y., Kainuma, R., and Ishida, k. "Feasibility of Cu-Al-Mn Superelastic Alloy Bars as Reinforcement Elements in Concrete Beams," *Smart Materials and Structures*, V. 22, No. 2, 2013, 15 pp.
- [6] Varela, S. and Saiidi, M.S., "Experimental Study on Seismically Resilient Two-Span Bridge Models Designed for Disassembly," *Journal of Earthquake Engineering*, V. 23, No. 1, 2019, pp. 72-111, DOI: 10.1080/13632469.2017.1309724.
- [7] Atanackovic, T. and Achenbach, M., "Moment-Curvature Relations for a Pseudoelastic Beam," *Continuum Mechanics and Thermodynamics*, V. 1, 1989, pp. 73-80.
- [8] Graesser, E.J. and Cozzarelli, F.A., "Shape-Memory Alloys as New Materials for Aseismic Isolation," *Journal of Engineering Mechanics*, V. 117, No. 11, 1991, pp. 2590-608.
- [9] Auricchio, F. and Sacco, E., "A Superelastic Shape-Memory-Alloy Beam Model," *Journal of Intelligent Material Systems and Structures*, V. 8, 1997, pp. 489-501.
- [10] Tazarv, M. and Saiidi, M.S., "Reinforcing NiTi Superelastic SMA for Concrete Structures," *Journal of Structural Engineering*, ASCE, DOI: 10.1061/(ASCE)ST.1943-541X.0001176, 2014, 10 pp.
- [11] DesRoches, R. and Smith, B., "Shape Memory Alloys in Seismic Resistant Design and Retrofit: A Critical Review of their Potential and Limitations," *Journal of Earthquake Engineering*, V. 7, No. 3, 2003, pp. 1-15.
- [12] Wilson, J.C. and Wesolowsky, M.J., "Shape Memory Alloys for Seismic Response Modification: A State-of-the-Art Review," *Earthquake Spectra*, V. 21, No. 2, 2005, pp. 569-601.

- [13] Song, G., Ma, N. and Li, H.N., “Applications of Shape Memory Alloys in Civil Structures,” *Engineering Structures*, V. 28, 2006, pp. 1266-1274.
- [14] Alam, M.S., Youssef, M.A. and Nehdi, M., “Utilizing Shape Memory Alloys to Enhance the Performance and Safety of Civil Infrastructures: a Review,” *Canadian Journal of Civil Engineering*, V. 34, 2007, pp. 1075-1086.
- [15] Dong, J., Cai, C.S. and Okeil, A.M., “Overview of Potential and Existing Applications of Shape Memory Alloys in Bridges,” *Journal of Bridge Engineering*, V. 16, No. 2, 2011, pp. 305-315.
- [16] Johnson, R., Padgett, J.E., Maragakis, M.E., DesRoches, R., and Saiidi, M.S., “Large Scale Testing of Nitinol Shape Memory Alloy Devices for Retrofitting of Bridges,” *Smart Materials and Structures*, V. 17, No. 3, 2008, 10 pp.
- [17] Andrawes, B., Shin, M., and Wierschem, N., “Active Confinement of Reinforced Concrete Bridge Columns Using Shape Memory Alloys,” *Journal of Bridge Engineering*, ASCE, V. 15, No. 1, 2010, pp. 81-89.
- [18] Wierschem, N. and Andrawes, B., “Superelastic SMA-FRP Composite Reinforcement for Concrete Structures,” *Smart Materials and Structures*, V. 19, 2010, 13 pp.
- [19] Ayoub, C., Saiidi, M.S., and Itani, A., “A Study of Shape-Memory Alloy-Reinforced Beams and Cubes,” Report No. CCEER-03-7, Center for Civil Engineering Earthquake Research, Dept. of Civil Engineering, Univ. of Nevada, Reno, NV, 2003.
- [20] Saiidi, M.S., Sadrossadat-Zadeh, M., Ayoub, C., and Itani, A., “Pilot Study of Behavior of Concrete Beams Reinforced with Shape Memory Alloys,” *Journal of Materials in Civil Engineering*, ASCE, V. 19, No. 6, 2007, pp. 454-461.
- [21] Saiidi, M.S. and Wang H., “Exploratory Study of Seismic Response of Concrete Columns with Shape Memory Alloys Reinforcement,” *ACI Structural Journal*, V. 103, No. 3, 2006, pp. 436-443.
- [22]. Youssef, M.A., Alam, M.S. and Nehdi, M., “Experimental Investigation on the Seismic Behavior of Beam-Column Joints Reinforced with Superelastic Shape Memory Alloys,” *Journal of Earthquake Engineering*, V. 12, No. 7, 2008, pp. 1205-1222.
- [23] Saiidi, M.S., O’Brien, M. and Sadrossadat-Zadeh, M., “Cyclic Response of Concrete Bridge Columns Using Superelastic Nitinol and Bendable Concrete,” *ACI Structural Journal*, V. 106, No. 1, 2009, pp. 69-77.
- [24] Cruz Noguez C.A. and Saiidi, M.S., “Shake Table Studies of a 4-Span Bridge Model with Advanced Materials,” *Journal of Structural Engineering*, ASCE, V. 138, No. 2, 2012, pp. 183-192.
- [25] Tazarv, M. and Saiidi, M.S., “Low-Damage Precast Columns for Accelerated Bridge Construction in High Seismic Zones,” *Journal of Bridge Engineering*, ASCE, DOI: 10.1061/(ASCE)BE.1943-5592.0000806, V. 21, No. 3, 2015, 13 pp.
- [26] AASHTO SGS, “AASHTO Guide Specifications for LRFD Seismic Bridge Design,” Washington, DC: American Association of State Highway and Transportation Officials, 2011.
- [27] Li, V.C., “Engineered Cementitious Composites (ECC): Material, Structural, and Durability Performance,” in *Concrete Construction Engineering Handbook*, Chapter 24, Ed. E. Nawy: published by CRC Press, 2008.
- [28] Kawashima, K., Zafra, R.G., Sasaki, T., Kajiwara, K., and Nakayama, M., “Effect of Polypropylene Fiber Reinforced Cement Composite and Steel Fiber Reinforced Concrete

- for Enhancing the Seismic Performance of Bridge Columns,” *Journal of Earthquake Engineering*, V. 15, No. 8, 2011, pp. 1194-1211.
- [29] Kawashima, K., Zafra, R.G., Sasaki, T., Kajiwara, K., Nakayama, M., Unjoh, S., Sakai, J., Kosa, K., Takahashi, Y., and Yabe, M., “Seismic Performance of a Full-Size Polypropylene Fiber-Reinforced Cement Composite Bridge Column Based on E-Defense Shake Table Experiments,” *Journal of Earthquake Engineering*, V. 16, No. 4, 2012, pp. 463-495.
- [30] Fischer, G. and Li, V.C., “Deformation Behavior of Fiber-Reinforced Polymer Reinforced Engineered Cementitious Composite (ECC) Flexural Members under Reversed Cyclic Loading Conditions,” *ACI Structural Journal*, V. 100, No. 1, 2003, pp. 25-35.
- [31] Motaref, S., Saiidi, M.S., and Sanders, D., “Seismic Response of Precast Bridge Columns with Energy Dissipating Joints,” Center for Civil Engineering Earthquake Research, Department of Civil and Environmental Engineering, University of Nevada, Reno, Report No. CCEER-11-01. 2011.
- [32] Nakashoji, B. and Saiidi, M.S., “Seismic Performance of Square Nickel-Titanium Reinforced ECC Columns with Headed Couplers,” Center For Civil Engineering Earthquake Research, Department Of Civil and Environmental Engineering, University of Nevada, Reno, Nevada, Report No. CCEER-14-05, 2014, 252 pp.
- [33] Aviram, A., Stojadinovic, B., and Parra-Montesinos, G.J., “High-Performance Fiber-Reinforced Concrete Bridge Columns under Bidirectional Cyclic Loading,” *ACI Structural Journal*, V. 111, No. 2, 2014, pp. 303-312.
- [34] Panagiotou, M., Trono, W., Jen, G., Kumar, P., and Ostertag, C.P., “Experimental Seismic Response of Hybrid Fiber-Reinforced Concrete Bridge Columns with Novel Longitudinal Reinforcement Detailing,” *Journal of Bridge Engineering*, ASCE, ISSN 1084-0702/04014090(12), 2014, 12 pp.
- [35] Mehrsoroush, A. and Saiidi, M.S., “Cyclic Response of Precast Bridge Piers with Novel Column-Base Pipe Pins and Pocket Cap Beam Connections,” *Journal of Bridge Engineering*, ASCE, V. 21, No. 4, 2016, 13 pp.
- [36] JSCE Concrete Library 127, “Recommendations for Design and Construction of High Performance Fiber Reinforced Cement Composites with Multiple Fine Cracks (HPFRCC),” Japan Society of Civil Engineers, 2008.
- [37] Tazarv, M. and Saiidi, M.S., “Analytical Studies of the Seismic Performance of a Full-Scale SMA-Reinforced Bridge Column,” *International Journal of Bridge Engineering*, V. 1, No. 1, 2013, pp. 37-50.
- [38] Tazarv, M. and Saiidi, M.S., “Next Generation of Bridge Columns for Accelerated Bridge Construction in High Seismic Zones,” Center For Civil Engineering Earthquake Research, Department of Civil and Environmental Engineering, University of Nevada, Reno, Nevada, Report No. CCEER-14-06, 2014, 400 pp.
- [39] Varela, S. and Saiidi, M.S., “Resilient Deconstructible Columns for Accelerated Bridge Construction in Seismically Active Areas,” *Journal of Intelligent Material Systems and Structures*, V. 28, No. 13, 2017, pp. 1751-1774.
- [40] Saiidi, M.S., Tazarv, M., Varela, S., Bennion, S., Marsh, M.L., Ghorbani, I., Murphy, T.M., “Seismic Evaluation of Bridge Columns with Energy Dissipating Mechanisms, Volume 1: Research Overview and Volume 2: Guidelines,” National Academies of Sciences, Engineering, and Medicine, NCHRP Report No. 864, Washington, DC: The National Academies Press. <https://doi.org/10.17226/24985>, 2017.

- [41] Hosseini, F., Gencturk, B., Lahpour, S., and Ibague Gil, D., “An Experimental Investigation of Innovative Bridge Columns with Engineered Cementitious Composites and Cu-Al-Mn Super-elastic Alloys,” *Smart Materials and Structures*, V. 24, No. 8, 2015, 16 pp., DOI:10.1088/0964-1726/24/8/085029.
- [42] Haber, Z.B., Saiidi, M.S., and Sanders, D.H., “Seismic Performance of Precast Columns with Mechanically Spliced Column-footing Connections,” *ACI Structural Journal*, V. 111, No. 3, 2014, pp. 639-650.
- [43] OpenSees, “Open System for Earthquake Engineering Simulations,” Version 2.4.1, Berkeley, CA, 2013, Available online: <http://opensees.berkeley.edu>.
- [44] Billah, A.H.M.M, and Alam, S.M., “Damping-Ductility Relationship for Performance Based Seismic Design of Shape Memory Alloy Reinforced Concrete Bridge Pier,” *The Proceeding of 2015 Structures Congress, ASCE*, 2015, pp. 474-484.
- [45] Billah, A.H.M.M, and Alam, S.M., “Performance-Based Seismic Design of Shape Memory Alloy-Reinforced Concrete Bridge Piers. I: Development of Performance-Based Damage States,” *Journal of Structural Engineering, ASCE*, V. 142, No. 12, 04016140, 2016, 13 pp.
- [46] Dwairi, H.M., Kowalsky, M.J., and Nau, J.M., “Equivalent Damping in Support of Direct Displacement-Based Design,” *Journal of Earthquake Engineering*, V. 11, No. 4, 2007, pp. 512-530.
- [47] Priestley, M.J.N., Calvi, G.M., and Kowalski, M.J., “Displacement-based seismic design of structures,” *IUSS press, Pavia*, 2007, 721 pp.
- [48] Seismosoft. (2013). *SeismoArtif v2.1-A Computer Program for Generating Artificial Earthquake Accelerograms Matched to a Specific Target Response Spectrum*, 2013, Available from <http://www.seismosoft.com>.
- [49] AASHTO LRFD, “AASHTO LRFD Bridge Design Specifications,” Washington, DC: American Association of State Highway and Transportation Officials, 2017.
- [50] Tazarv, M. and Saiidi, M.S., “Seismic Design of Bridge Columns Incorporating Mechanical Bar Splices in Plastic Hinge Regions,” *Engineering Structures*, DOI: 10.1016/j.engstruct.2016.06.041, V. 124, 2016, pp. 507-520.
- [51] Baker, T., Saiidi, M.S., Nakashoji, B., Bingle, J., Moore, T., and Khaleghi, B., “Precast concrete spliced-girder bridge in Washington State using superelastic materials in bridge columns to improve seismic resiliency: From research to practice,” *PCI Journal*, Jan.-Feb. 2018, pp. 57-71.

Table 1–Minimum and expected tensile NiTi Superelastic SMA bar mechanical properties [10]

Parameter	Minimum ^(a)	Expected ^(b)
Austenite modulus, k_1	4500 <i>ksi</i> (31025 <i>MPa</i>)	5500 <i>ksi</i> (37900 <i>MPa</i>)
Post yield stiffness, k_2	--	250 <i>ksi</i> (1725 <i>MPa</i>)
Austenite yield strength, f_y	45 <i>ksi</i> (310 <i>MPa</i>)	55 <i>ksi</i> (380 <i>MPa</i>)
Lower plateau stress factor, β	0.45	0.65
Recoverable superelastic strain, ϵ_r	6%	6%
Secondary post-yield stiffness ratio, α	--	0.3
Ultimate strain, ϵ_u	10%	10%

Note: ^(a) to be used in material production and for non-seismic design (e.g. service limit state).

^(b) to be used in seismic design of SMA-reinforced concrete members.

Source: Tazarv and Saiidi ¹⁰

Table 2–Bridge column drift ratio demand requirements

Member	Conventional Columns	Novel Columns
Single-column bents	$\mu_D \leq 5$	Aspect Ratio 4: $\delta_D \leq 3.6\Omega$
		Aspect Ratio 6: $\delta_D \leq 5.1\Omega$
		Aspect Ratio 8: $\delta_D \leq 6.4\Omega$
Multiple-column bents	$\mu_D \leq 6$	Aspect Ratio 4: $\delta_D \leq 4.4\Omega$
		Aspect Ratio 6: $\delta_D \leq 6.2\Omega$
		Aspect Ratio 8: $\delta_D \leq 7.8\Omega$

Note: “ δ_D ” is the drift ratio demand (%) and “ μ_D ” is the displacement ductility demand

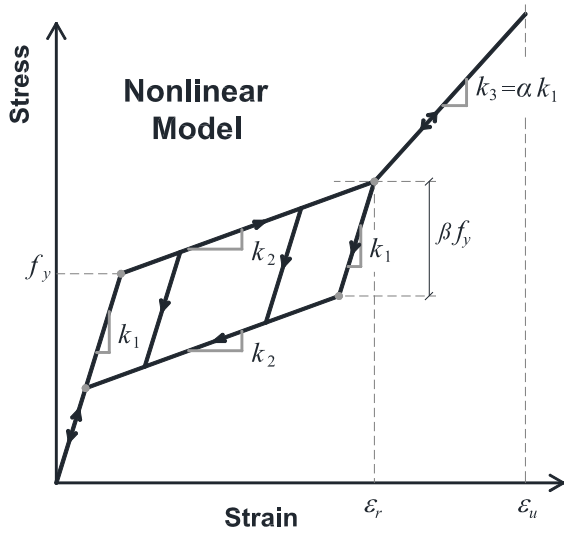
Use linear interpolation for intermediate aspect ratios

Table 3–Minimum bridge column drift ratio capacity requirements

Member	Conventional Columns	Novel Columns
Single- or multi-column bents	$\mu_c \geq 3$	Aspect Ratio 4: $\delta_c \geq 2.0\%$
		Aspect Ratio 6: $\delta_c \geq 2.85\%$
		Aspect Ratio 8: $\delta_c \geq 3.60\%$

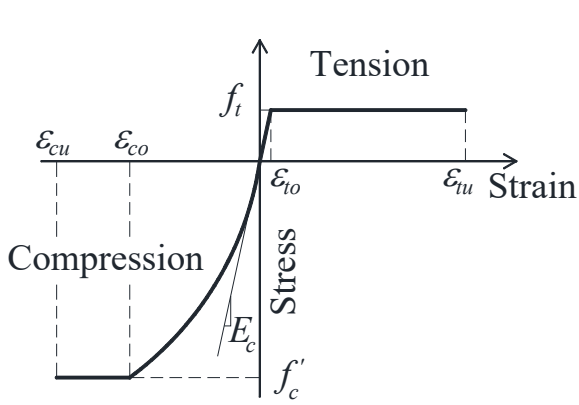
Note: “ δ_c ” is the drift ratio capacity (%) and “ μ_c ” is the displacement ductility capacity

Use linear interpolation for intermediate aspect ratios



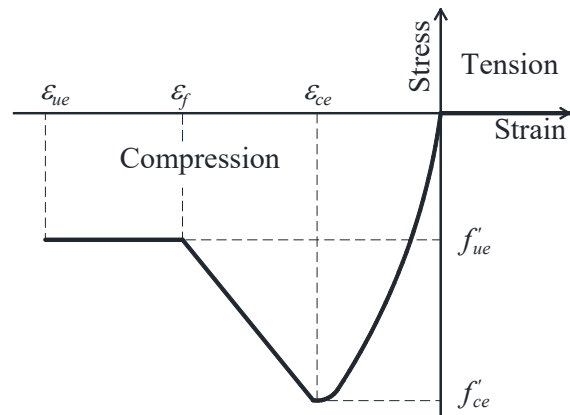
Source: Tazarv and Saiidi¹⁰

Figure 1–Superelastic SMA material model [10]



(a) Unconfined ECC³⁶

Figure 2–ECC material models



(b) Steel Confined ECC³¹

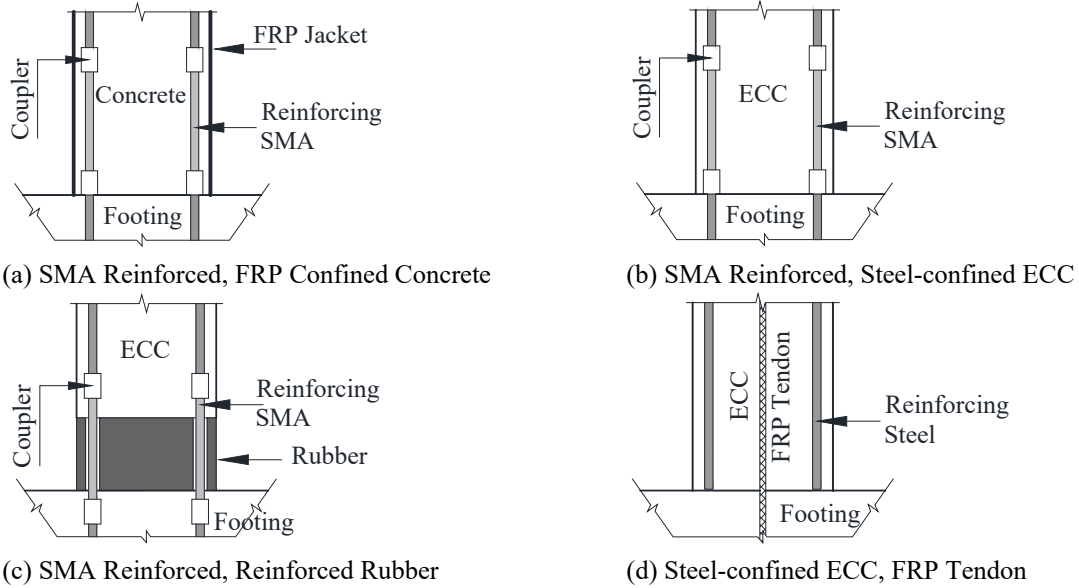


Figure 3—Novel bridge columns incorporating SMA and/or ECC

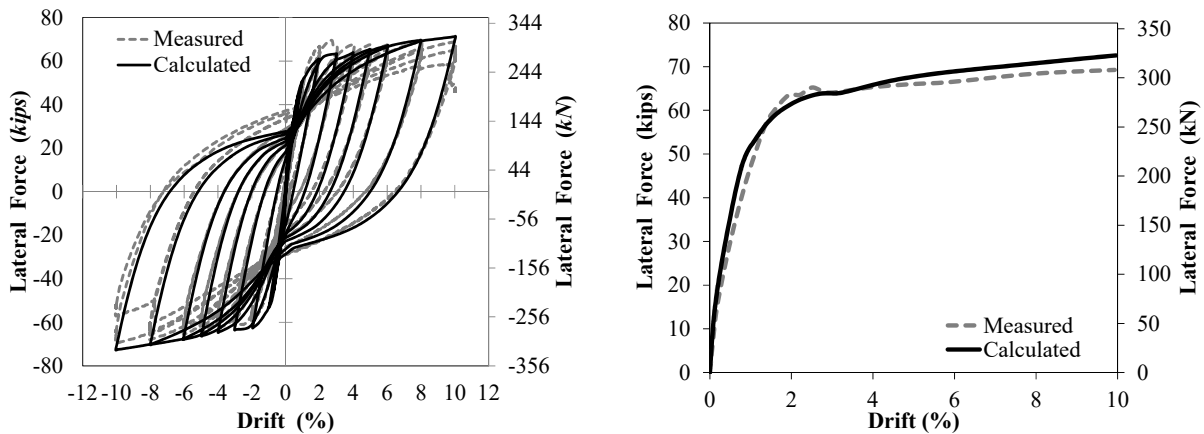


Figure 4—Model verification for a half-scale conventional RC bridge column